ISSN 2336-3193
DOI: 10.2478/cszma-2025-0008

Published: online November 2025, print November 2025

Predictive Maps for the Species *Heracleum mantegazzianum* for the periods 2011–2040 and 2041–2070 in central Europe.

Lukáš Číhal

Predictive Maps for the Species *Heracleum mantegazzianum* for the periods 2011–2040 and 2041–2070 in central Europe. – Acta Mus. Siles. Sci. Natur. 74: 123–135, 2025.

Abstract: This study applies MaxEnt modeling to predict the future distribution of the invasive plant *Heracleum mantegazzianum* in Central Europe (mainly the Czech Republic, Slovakia, Austria, Germany, and Poland) for two time periods, 2011–2040 and 2041–2070. A baseline model was also developed for the historical period 1980–2010 to serve as a reference for comparison with future projections. High-resolution CHELSA bioclimatic variables were combined with occurrence records from the Species Occurrence Database (NDOP) of the Nature Conservation Agency of the Czech Republic (AOPK ČR) and from the Global Biodiversity Information Facility (GBIF), an international open access database of biodiversity records, to create species distribution models. The models achieved fair to good predictive performance and revealed clear spatial shifts between the historical baseline (1980–2010) and future projections for 2011–2040 and 2041–2070. Areas with high habitat suitability are expected to expand into regions that were only moderately suitable in the past, with southern and western Germany showing the most pronounced increases. Differences between low emission (SSP126) and high emission (SSP585) climate scenarios were limited, suggesting that the species occupies a relatively stable climatic niche. Environmental novelty analyses identified regions of increasing uncertainty due to emerging climatic conditions, highlighting the need for cautious interpretation of projections for 2041–2070. These results highlight priority areas for monitoring and management and demonstrate how climate change may drive the future spread of this invasive species.

Keywords: invasive species, *Heracleum mantegazzianum*, species distribution modeling, MaxEnt, Central Europe, climate change, habitat suitability

Introduction

Non-native and invasive plant species have been companions to humankind for thousands of years, however, this issue has become increasingly pressing in recent times (Lockwood et al. 2013). Today, with global travel being more widespread than ever, it has become common for plants that would not naturally cross geographical and other barriers to colonize new, non–native territories. This phenomenon does not spare Central Europe, where hundreds of non–native plant species can be found in the wild, some of which exhibit invasive behavior.

H. mantegazzianum is a monocarpic perennial native to the Caucasus, where it occurs from lowland river valleys up to subalpine tall herb communities, favoring nutrient–rich, moist soils and open to semi–shaded conditions (Pyšek et al. 2007a). In its introduced European range, it predominantly colonizes disturbed riparian habitats, abandoned grasslands, roadsides, and forest edges, where its rapid growth and high canopy production allow it to suppress native vegetation and form monospecific stands (Thiele & Otte 2007). Its regeneration relies entirely on seed production; dormancy is broken by cold stratification, and the seed bank is short-lived, rarely persisting beyond a few years (Moravcová et al. 2006). Successful invasion is strongly linked to high propagule pressure, dispersal along river corridors, and anthropogenic disturbance, while shaded habitats with developed woody cover limit establishment (Pyšek et al. 2007b, Pyšek et al. 2009).

Material and Methods

This study aims to predict the interaction between the environment and invasive plants as a dynamic system evolving across space and time, using predictive models. To develop these models, methods utilizing machine learning were chosen. These approaches employ algorithms and techniques that enable a computer system to learn. The algorithm used, MaxEnt, is a machine learning method (Phillips & Dudík, 2008) that calculates certain values for each pixel of the studied area based on input data. These values (probabilities) are scaled on a scale from 0 to 1 and represent an index of relative suitability (Anderson & Gonzalez, 2011), meaning they identify areas similar to those where the species already occurs (Pearson et al., 2007) In this study, these represent areas suitable for the studied species.

For the calculation of individual models, MaxEnt software version 3.4.4 (Phillips et al., n.d.) was used. For data preparation and processing of individual layers, the programs R version 4.4.2 (R Core Team 2024) and QGIS version 3.34 'Prizren' (QGIS Development Team 2024) were used.

Species distribution models calibrated for the period 2011–2040 were projected onto future environmental layers (2041–2070) using the function kuenm_mod (Cobos et al. 2019) in R. This approach allows transferring the fitted MaxEnt models to new climatic conditions without refitting, resulting in suitability maps for future scenarios.

Geographical Study Area

The study area encompasses a portion of Central Europe, defined by a geographical range spanning from 46.3167° N to 55.0500° N latitude and from 5.8667° E to 24.1333° E longitude. The primary focus of the study is on the Czech Republic, Slovakia and Austria, Germany, and Poland. The same area was used for model creation and their projection, which eliminated potential issues with projecting the models onto different territories (for a detailed overview of the study area, see the Fig. 1).

Geographical data

The source of input data was the Species Occurrence Database NDOP (AOPK ČR 2025). These data were downloaded using the ndop_download function from the rndop package (Kaláb 2024). The data were cleaned, retaining only records with GPS coordinates and collection dates.

Additional occurrence data were obtained from the Global Biodiversity Information Facility (GBIF.org, accessed 2025) using the sp_occurrence function from the geodata package (Hijmans et al., 2023). The data were cleaned with the clean_coordinates function from the CoordinateCleaner package (Zizka et al., 2019) to remove erroneous or imprecise records.

The combined dataset was divided into two time periods, 1980–2010 and 2011–2025 (up to January 2025) to match the corresponding environmental layers. To reduce spatial autocorrelation and redundancy in the occurrence data, each subset was filtered using the thin function from the R package spThin (Aiello-Lammens et al., 2015), evaluating three thinning distances: 1, 3, and 5 km.

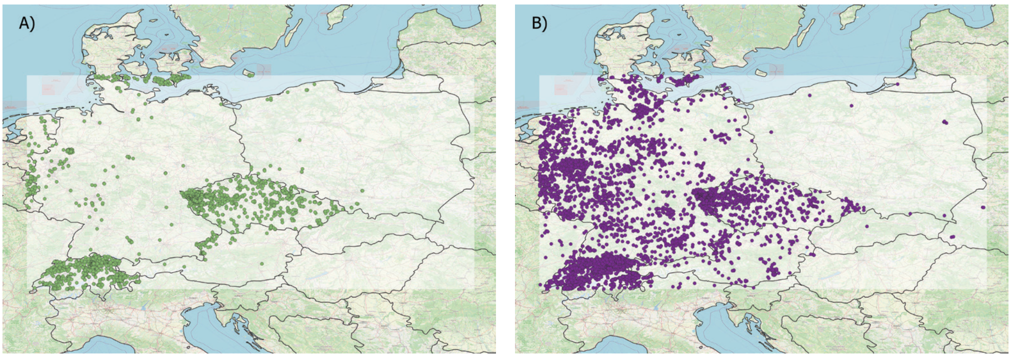

Fig. 1: Geographical distribution of *H. mantegazzianum* after thinning (1 km). **(A)** Records for 1980–2010 (green dots); **(B)** records for 2011–2025 (purple dots). The study area is highlighted with a white rectangle. Basemap © OpenStreetMap contributors (2024).

Selection of Background Points for MaxEnt Modeling

To ensure adequate representation of the environmental space in the MaxEnt model for *H. mantegazzianum*, the number of background points was evaluated to balance model performance and computational efficiency (Elith et al. 2011).

The study area in Central Europe, represented by a raster with approximately 2.3 million cells (2192 × 1048, ~1 km resolution), necessitated a sufficient number of background points to capture environmental variability. Seven quantities were tested: 10,000, 15,000, 20,000, 25,000, 30,000, 35,000, and 40,000 background points.

Environmental variables

Nineteen high-resolution (30 arc seconds, ~1 km) bioclimatic variables from the CHELSA 2.1 dataset (Climatologies at High Resolution for Earth's Land Surface Areas) were initially evaluated for constructing the MaxEnt model for the reference period 1980–2010 (Karger et al., 2017; Karger et al., 2020). Variables 8, 9, 18, and 19 were excluded due to potential redundancy or limited biological relevance (Booth, 2022).

Environmental layers for 2011–2040 and 2041–2070 were also obtained from CHELSA, derived from CMIP6 global climate models (GCMs) GFDL-ESM4 (NOAA, Geophysical Fluid Dynamics Laboratory, Princeton, NJ, USA) and IPSL-CM6A-LR (Pierre Simon Laplace Institute, Paris, France), under two Shared Socioeconomic Pathways (SSPs 126 and 585) representing contrasting trajectories of economy, demographics, technology, and environmental policy (O'Neill et al., 2017).

To ensure robust and comparable MaxEnt models across scenarios, a systematic variable selection process was applied to remove collinear predictors. Variance Inflation Factor (VIF) analysis was conducted using the usdm package in R (Naimi et al., 2014), applying the vifstep function to the remaining 15 bioclimatic variables from the reference period. Variables with VIF > 10 were iteratively removed until all remaining predictors were below the threshold.

In total, 45 input layers were used to generate maps for all scenarios, comprising five selected bioclimatic variables for each scenario–time combination: CHELSA (1980–2010), GFDL-ESM4 SSP126 (2011–2040), GFDL-ESM4 SSP585 (2011–2040), GFDL-ESM4 SSP126 (2041–2070), GFDL-ESM4 SSP585 (2041–2070), IPSL-CM6A-LR SSP126 (2011–2040), IPSL-CM6A-LR SSP585 (2011–2040), IPSL-CM6A-LR SSP126 (2041–2070), and IPSL-CM6A-LR SSP585 (2041–2070).

For modeling, combinations of environmental variables with a minimum of four variables per set were generated using the kuenm_varcomb function from the kuenm package (Cobos et al., 2019), resulting in six different layer sets for each scenario (Tab. 1).

Tab. 1: Environmental Variables Contained in Each Set.

Set Number	**Variables**
Set_1	bio1, bio3, bio14, bio15
Set_2	bio1, bio4, bio14, bio15
Set_3	bio1, bio3, bio4, bio14
Set_4	bio1, bio3, bio4, bio15
Set_5	bio3, bio4, bio14, bio15
Set_6	bio1, bio3, bio4, bio14, bio15

Model calibration

Calibration was performed using the kuenm_cal function from the kuenm package (Cobos et al. 2019) in R. A total of 150 candidate models were evaluated for each climate model and socioeconomic scenario, with parameters reflecting all combinations of 5 regularization parameter settings, 5 feature class combinations, and 6 different environmental variable sets (Tab. 2). In total, 1350 models were created for all combinations of models, scenarios, variable sets and parameters.

Model Evaluation

Calibrated model evaluation was conducted using the kuenm_ceval function from the kuenm R package (Cobos et al., 2019). This procedure generated 150 candidate models (combinations of regularization multipliers, feature classes, and variable sets) and evaluated them using two main criteria: omission rate (OR) at a 5% threshold and the corrected

Akaike Information Criterion (AICc). Model selection was performed with the OR_AICc criterion, which prioritizes models with low omission rates and, among those, selects the one with the lowest AICc value, balancing predictive accuracy with model parsimony.

To assess model robustness, performance metrics were based on 50 iterations of random data partitioning (cross–validation). For the final models, we additionally report the Area Under the Curve (AUC) evaluation scores. Following Swets (1988), AUC values < 0.6 were interpreted as poor performance, 0.6–0.7 as weak, 0.7–0.8 as fair, 0.8–0.9 as good, and 0.9–1.0 as excellent.

Final models were generated using the kuenm_mod function (Cobos et al., 2019), with the best configurations identified through the above evaluation procedure.

Tab. 2: Specific values of parameters for Creating MaxEnt Models.

Parameter	**Values**
Regularization multipliers	0,1; 0,4; 0,7; 1; 2
Feature classes	l, lq, lqp, lqpt, lqpth
Sets of environmental layer combinations	Set_1, Set_2, Set_3, Set_4, Set_5, Set_6

Environmental Novelty Analysis

To assess environmental novelty between a 2011–2040 period and future climate projections (2041–2070), we applied a Principal Component Analysis (PCA)–based approach (Mesgaran et al., 2014). This method was used to identify regions exhibiting extrapolation (Type I novelty, NT1) and regions with novel combinations of environmental variables (Type II novelty, NT2).

A random sample of 5,000 pixels was extracted from the 2011–2040 raster stacks to reduce computational demands while maintaining representativeness. Missing values were excluded, and the data were standardized (mean = 0, SD = 1) prior to PCA. The PCA transformed the original bioclimatic variables into a reduced set of orthogonal principal components (PCs), capturing the majority of variance. Both baseline (2011–2040) and future (2041–2070) data were projected into the same PC space to ensure comparability.

NT1 was determined by comparing each pixel's projected PC values to the baseline range (min–max). Pixels with any PC value outside this range were classified as NT1. NT2 was assessed using Mahalanobis distance 'in PC space, with pixels exceeding the 99th percentile of the baseline distance distribution flagged as NT2. The analysis was conducted only for the reprojected maps representing 2041–2070.

Results

For the final model creation, 2,504 records from the 1980–2010 period for CHELSA 1980–2010 environmental layers and 5,793 records from the 2011–2025 period for all 2011–2040 environmental layers were used (Tab. 3).

Tab. 3: Number of occurrence records from NDOP and GBIF databases.

	GBIF data	**NDOP data**	**combined before thinning**	**combined after thinning (1 km)**
1980–2010	6821	2588	9409	2504
2011–2025	21601	5014	26615	5793

For cleaning the data, the 1 km thinning parameter was chosen because it aligned with the approximately 1 km resolution of the environmental raster layers used in the MaxEnt model, preserving fine–scale environmental variability essential for modeling an invasive species in Central Europe‘s heterogeneous landscapes. Additionally, the 1 km filter retained more records from the original dataset, ensuring a robust dataset for model training and adequate representation of the species‘ environmental niche. MaxEnt models based on the 1 km thinned dataset outperformed those using the 3 and 5 km dataset, achieving a higher Mean AUC ratio, lower omission rates at the 5% threshold, and fewer parameters, indicating better discriminatory power, fewer false negatives, and a simpler model less prone to overfitting. Thus, the 1 km thinning parameter effectively balanced the reduction of spatial autocorrelation with the preservation of sufficient occurrence data, supporting robust and generalizable MaxEnt models for predicting the future spread of the studied species.

The cleaned and unified species occurrence data were divided into training (70%) and testing (30%) datasets using the kuenm_occsplit function from the kuenm R package (Cobos et al., 2019) with a random split method. This partitioning facilitated model calibration with the training data and independent evaluation of model performance using the test data.

For choosing the background points, after testing of different quantitie of background points, models with 25,000 and 30,000 points were closely compared due to their similar performance metrics, with 30,000 background points ultimately selected as the optimal choice. This decision was based on the models with 30,000 points achieving a slightly lower omission rate at the 5% threshold, indicating fewer false negatives, which is critical for predicting the spread of an invasive species. Additionally, the models with 30,000 points utilized higher regularization coefficients and fewer parameters, suggesting a simpler model with improved generalization, essential for robust predictions under future climate scenarios up to 2070. The 30,000 points, representing approximately 1.3 % of the total raster cells, provided robust coverage of the heterogeneous environmental gradients in the study area while maintaining computational feasibility. Thus, 30,000 background points were chosen to optimize model accuracy, simplicity, and generalizability for predicting the future distribution of *H. mantegazzianum*.

The vifstep analysis for reducing collinear variables was used and identified 10 collinear variables (bio2, bio5, bio6, bio7, bio10, bio11, bio12, bio13, bio16, bio17), which were subsequently excluded. The remaining five non–collinear variables were bio1, bio3, bio4, bio14, and bio15. The Pearson correlation coefficients between these variables ranged from –0.07995802 (bio4 ~ bio1) to 0.5325936 (bio4 ~ bio15).

Based on these results, the following variables were selected for final modeling and map creation: bio1: mean annual air temperature, bio3: isothermality, bio4: temperature seasonality, bio14: precipitation amount of the driest month and bio15: precipitation seasonality.

For future climate scenarios these variables generally maintained acceptable VIF scores. Notably, bio14 occasionally exhibited higher VIF values (e.g., 8.985 in gfdl–esm4SSP585 2041–2070), but their overall stability during the reference period justified their inclusion across all timeframes.

The table below (Tab. 4) presents performance statistics for the final models selected based on the defined criteria. Models were evaluated using datasets for the 1980–2010 (n = 2504) and 2011–2040 (n = 5793) periods under different Shared Socioeconomic Pathways (SSP126, SSP585) and climate models (gfdl–esm4, ipsl–cm6a–lr). Reported performance measures include mean AUC, mean AUC ratio, omission rate at the 5% threshold, AICc, and the number of parameters. For the period 2041–2070, only AUC scores are reported, as models were not refitted for this time frame. Instead, the models trained on current species data and 2011–2040 environmental variables were reprojected onto the climate projections for 2041–2070, providing future suitability maps without recalibration.

Model configurations include regularization multipliers (e.g., M), feature classes (e.g., lqpth: linear, quadratic, product, threshold, hinge), and variable sets based on Tab. 2 explanations.

Tab. 4: Performance statistics for final models selected based on defined criteria.

Model	Model ConFiguration	Mean AUC	Mean AUC Ratio	Omission Rate at 5%	AICc	N Parameters
CHELSA 1980–2010	M_0.1_F_lqpth_ Set_6	0.845	1.610	0.049	67717.51	240
2011–2040_gfdl–esm4_SSP126	M_0.4_F_lqpth_ Set_3	0.778	1.419	0.049	160794.8	162
2011–2040_gfdl–esm4_SSP585	M_0.1_F_lqpt_ Set_6	0.793	1.446	0.05	159358.7	253
2011–2040_ipsl–cm6a–lr_ SSP126	M_0.1_F_lqpth_ Set_6	0.788	1.424	0.049	159966	293
2011–2040_ipsl–cm6a–lr_ SSP585	M_0.1_F_lqpth_ Set_6	0.788	1.439	0.05	160018.1	274
2041–2070_gfdl–esm4_SSP126	-	0.785	-	-	-	-
2041–2070_gfdl–esm4_SSP585	-	0.803	-	-	-	-
2041–2070_ipsl–cm6a–lr_ SSP126	-	0.798	-	-	-	-
2041–2070_ipsl–cm6a–lr_ SSP585	-	0.798	-	-	-	-

Predictive maps

The generated maps provide a better understanding of the ecological characteristics affecting the occurrence of invasive plant species and help identify areas that are most suitable for the species based on the models.

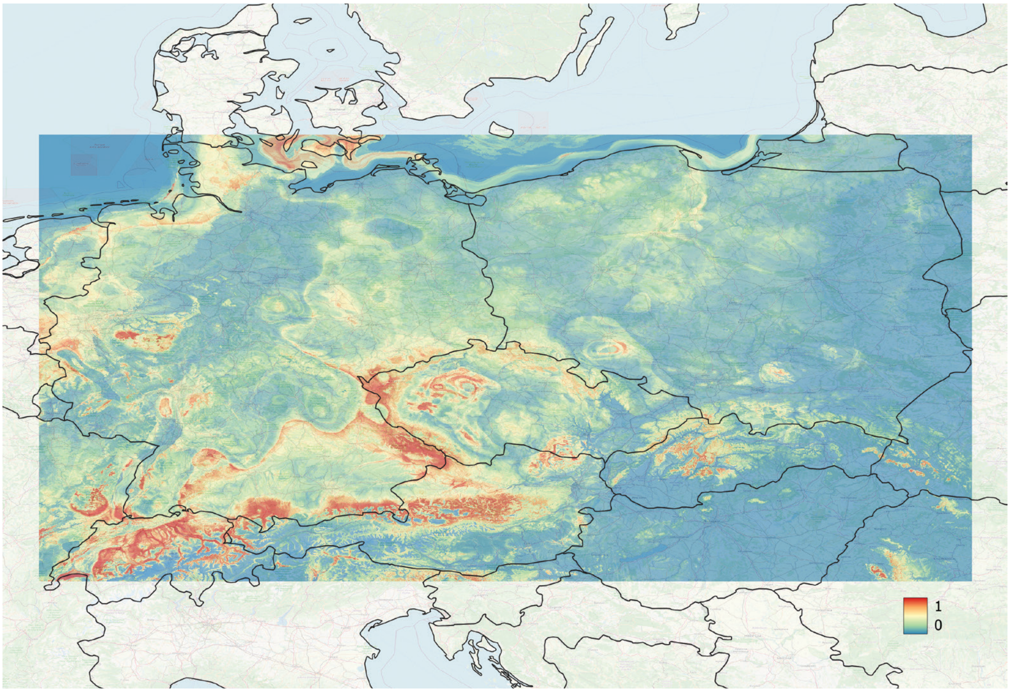

Fig. 2: Prediction map for the period 1980–2010, using the CHELSA dataset with a regularization multiplier of M_0.1, feature classes F_lqpth, and variable set Set_6. Basemap: © OpenStreetMap contributors (2024).

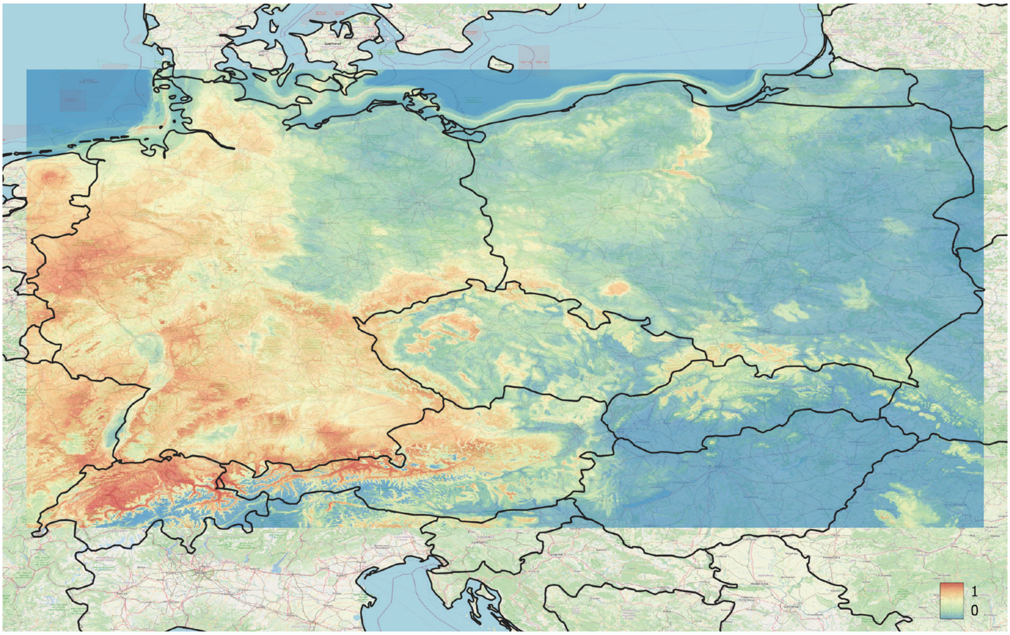

Fig. 3: Prediction map for the period 2011–2040, using the gfdl–esm4 climate model and SSP126 socio-economic scenario, with a regularization multiplier of M_0.4, feature classes F_lqpth, and variable set Set_3. Basemap: © OpenStreetMap contributors (2024).

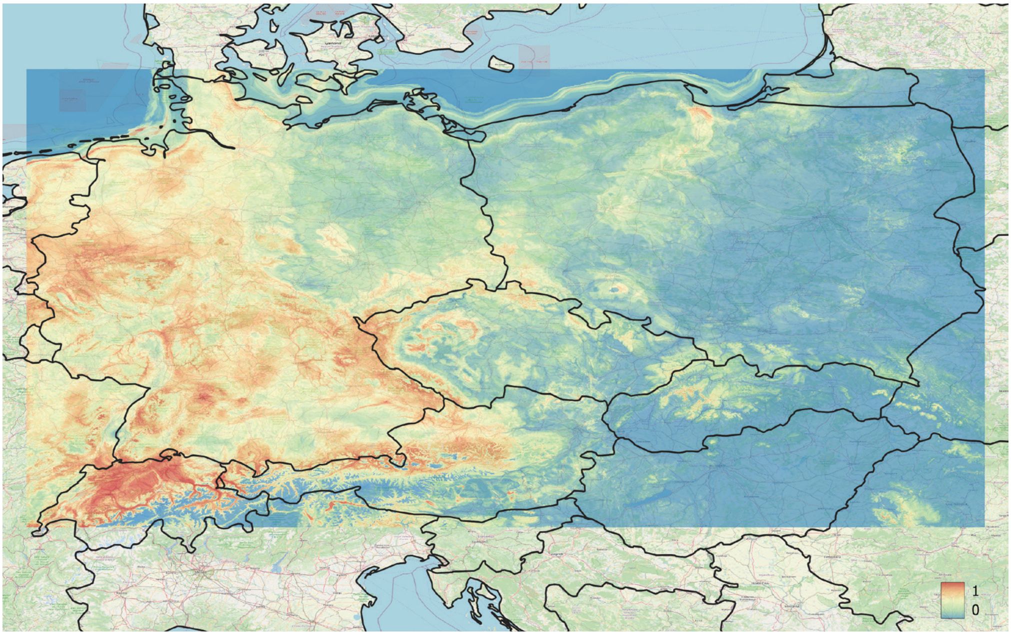

Fig. 4: Prediction map for the period 2011–2040, using the gfdl–esm4 climate model and SSP585 socio-economic scenario, with a regularization multiplier of M_0.1, feature classes F_lqpt, and variable set Set_6. Basemap: © OpenStreetMap contributors (2024).

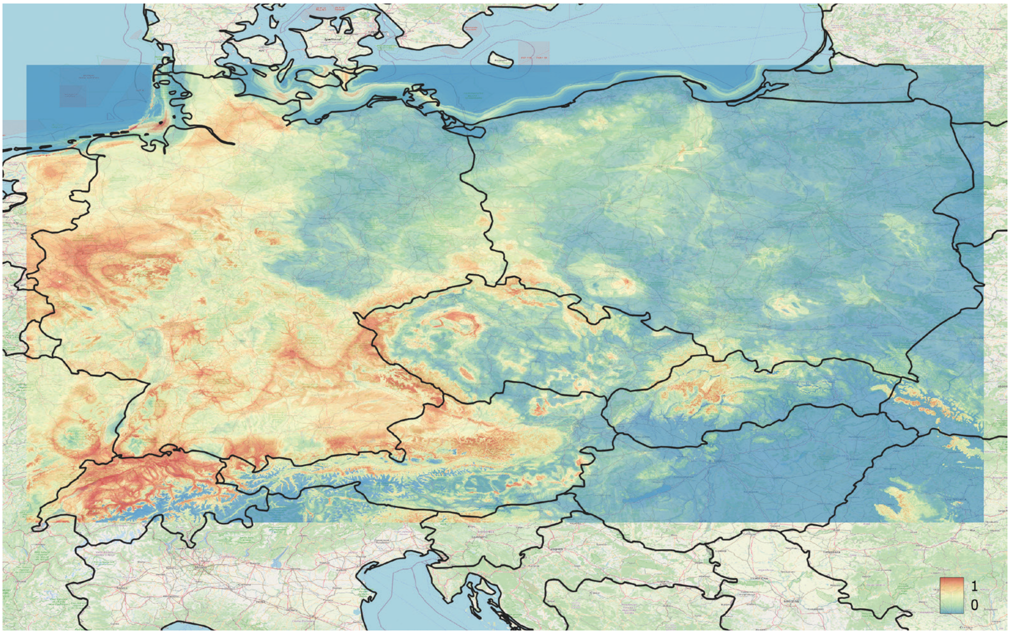

Fig. 5: Prediction map for the period 2011–2040, using the ipsl–cm6a–lr climate model and SSP126 socio-economic scenario, with a regularization multiplier of M_0.1, feature classes F_lqpth, and variable set Set_6. Basemap: © OpenStreetMap contributors (2024).

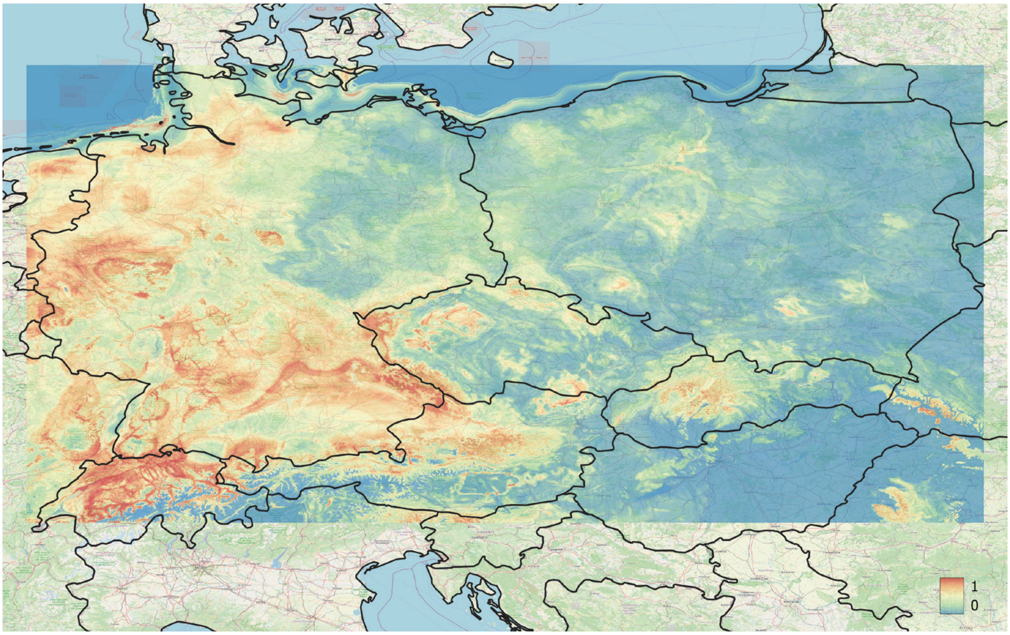

Fig. 6: Prediction map for the period 2011–2040, using the ipsl–cm6a–lr climate model and SSP585 socio-economic scenario, with a regularization multiplier of M_0.1, feature classes F_lqpth, and variable set Set_6. Basemap: © OpenStreetMap contributors (2024).

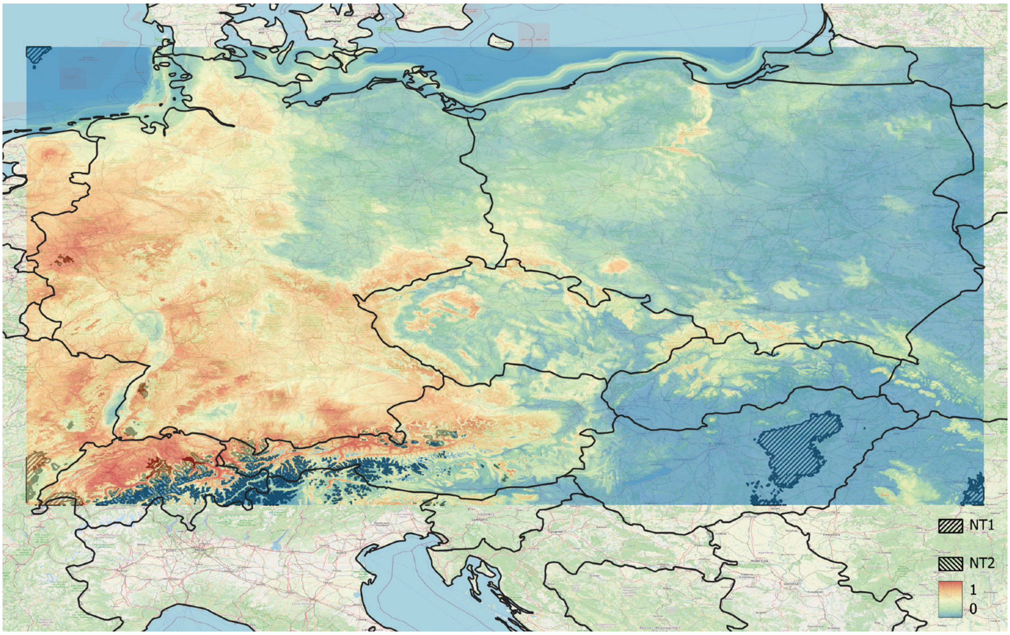

Fig. 7: Prediction map for the period 2041–2070, using the gfdl–esm4 climate model and SSP126 socio-economic scenario. M, F and Set are the same as 2011–2040, using the gfdl–esm4 climate model and SSP126 socio-economic scenario. Basemap: © OpenStreetMap contributors (2024).

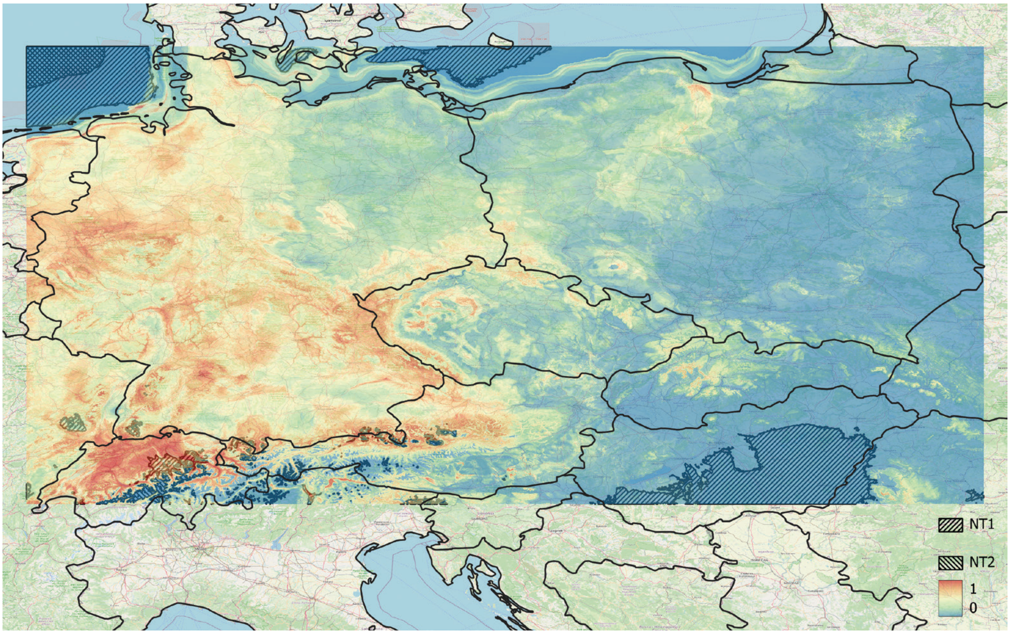

Fig. 8: Prediction map for the period 2041–2070, using the gfdl–esm4 climate model and SSP585 socio-economic scenario. M, F and Set are the same as 2011–2040, using the gfdl–esm4 climate model and SSP585 socio-economic scenari.o Basemap: © OpenStreetMap contributors (2024).

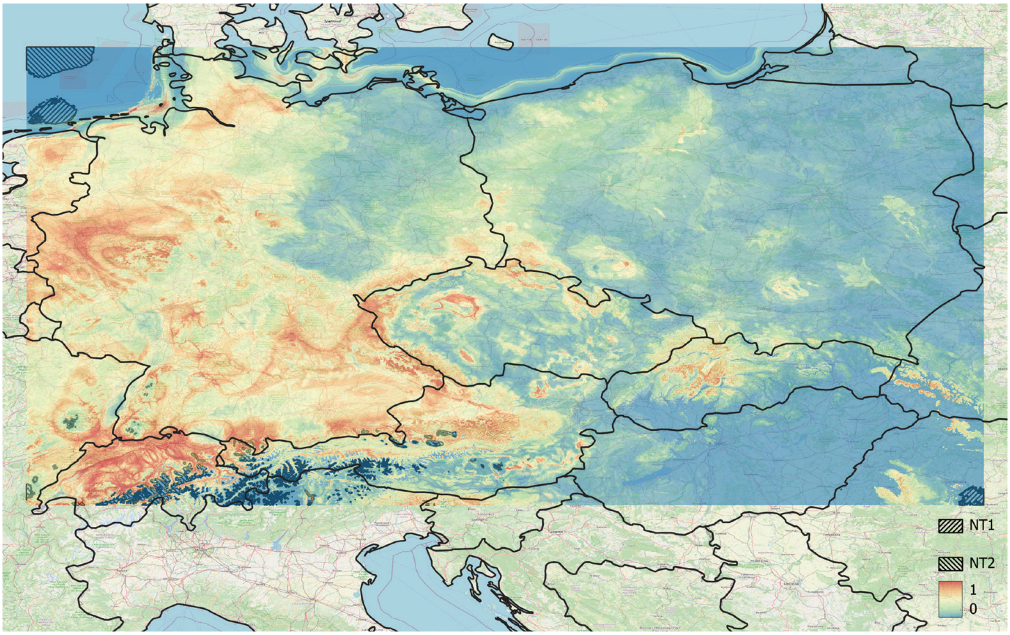

Fig. 9: Prediction map for the period 2041–2070, using the ipsl–cm6a–lr climate model and SSP126 socio-economic scenario. M, F and Set are the same as 2011–2040, using the ipsl–cm6a–lr climate model and SSP126 socio-economic scenario. Basemap: © OpenStreetMap contributors (2024).

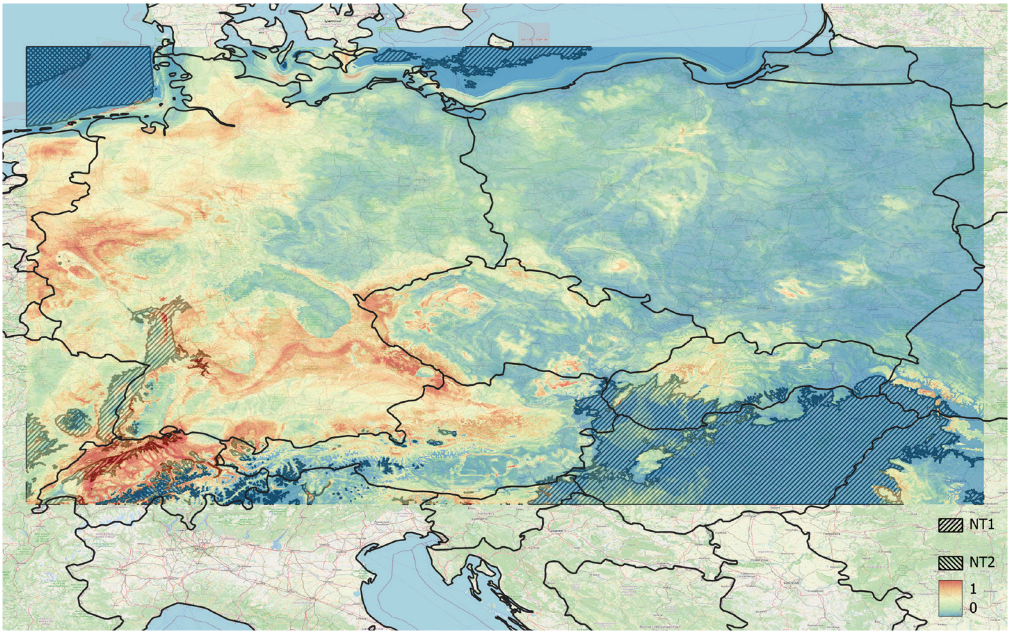

Fig. 10: Prediction map for the period 2041–2070, using the ipsl–cm6a–lr climate model and SSP585 socio-economic scenario. M, F and Set are the same as 2011–2040, using the ipsl–cm6a–lr climate model and SSP585 socio-economic scenario. Basemap: © OpenStreetMap contributors (2024).

The following maps display the probabilities for different scenarios. The color gradient ranges from blue (representing low probabilities, close to 0) to red (representing high probabilities, close to 1). For orientation, state borders are marked and background maps were provided by OpenStreetMap contributors (2024). When two factor combinations yield equivalent performance in a MaxEnt model, the model with a higher lqpth setting is displayed. In all cases, the differences were limited to the regularization multipliers (lqpt or lqpth settings) between models with the same performance.

Projected Distribution Dynamics of *H. mantegazzianum* in Central Europe

Predictive MaxEnt models suggest that the future distribution of *H. mantegazzianum* in Central Europe will expand, with particularly strong increases in southern and western Germany. These regions are projected to experience substantial gains in habitat suitability, both in extent and intensity.

Across both projected periods (2011–2040 and 2041–2070) and climate scenarios (SSP126 and SSP585), spatial distribution patterns remain largely consistent. Core areas of occurrence persist and expand under increasingly favorable climatic conditions. Differences between the low-emission (SSP126) and high-emission (SSP585) pathways are minimal with respect to both spatial extent and habitat suitability.

Temporal variation between the two future periods is also limited. However, projections indicate the emergence of regions of environmental novelty (NT1), especially in southern Austria, southern Slovakia, and most notably in Hungary. The presence of NT1 areas across the study region signals the development of climatic conditions not previously observed.

In summary, the findings point to a climate-driven redistribution of suitable habitats for *H. mantegazzianum*, with a clear trend toward broader spatial coverage across Central Europe under future climate conditions. This anticipated spread underscores the urgency of targeted monitoring and control efforts in the most affected regions.

Discussion

The predictive maps generated for *H. mantegazzianum* in Central Europe provide valuable insights into the species' potential distribution under current and future climate scenarios. Using the MaxEnt modeling framework with carefully selected environmental variables and occurrence data identified areas of high suitability for establishment across both future periods (2011–2040 and 2041–2070). The incorporation of high-resolution (~1 km) CHELSA 2.1 climate layers ensured that the models captured fine-scale environmental variability, which is critical for understanding the ecological dynamics of an invasive species in a heterogeneous region such as Central Europe.

The projections indicate particularly strong expansion in southern and western Germany, reflecting the species' capacity to exploit favorable climatic conditions. This expansion is likely driven by a combination of warmer temperatures (CHELSA_bio1 and bio4) and suitable precipitation regimes (bio14 and bio15), consistent with the ecological requirements of *H. mantegazzianum*. These regions, characterized by mild winters and adequate moisture, provide ideal conditions for establishment and spread. Importantly, the consistency of results across both SSP126 and SSP585 scenarios suggests a relatively stable climatic niche.

Environmental novelty analyses further revealed NT1 and NT2 areas, particularly in southern Austria, southern Slovakia, and Hungary. These regions represent novel climatic conditions and introduce greater uncertainty into predictions, underscoring the need for cautious interpretation and continued monitoring to validate future model outcomes.

The spatial patterns revealed by these maps provide a practical foundation for conservation and management planning. Areas of high climatic suitability should be prioritized for monitoring and control to prevent further spread of *H. mantegazzianum*. Proactive strategies that account for climate change impacts and encourage cross-border cooperation are essential, given the species' capacity to expand across national boundaries. As climate change continues to reshape environmental conditions, predictive tools such as these will play a critical role in anticipating and managing biological invasions, thereby supporting biodiversity conservation and ecosystem resilience in Central Europe.

While the models presented here rely exclusively on climatic predictors, it is important to acknowledge that other ecological and anthropogenic factors—such as soil properties, land use, habitat disturbance, and human-mediated dispersal—substantially influence realized distributions. Consequently, our projections should be interpreted as estimates of climatic potential rather than actual species distributions. Climate-only models inevitably simplify invasion dynamics, as they omit key local and regional drivers (Pearson & Dawson, 2003; Franklin, 2010).

At the same time, climate-based models offer distinct advantages. They provide a robust assessment of the fundamental climatic niche, minimize confounding influences from poorly documented non-climatic variables, and enable comparisons across broad spatial and temporal scales (Araújo & Peterson, 2012). Moreover, such models are widely used as a first approximation to identify areas at risk under future climate scenarios, offering a valuable baseline for conservation planning, invasion monitoring, and subsequent integration with more complex ecological and socioeconomic variables (Elith & Leathwick, 2009; Guisan & Thuiller, 2005).

Acknowledgments: This article was financially supported by the Ministry of Culture of the Czech Republic by institutional financing of long–term conceptual development of the research institution (the Silesian Museum, MK000100595).

References

Aiello–Lammens, M. E., Boria, R. A., Radosavljevic, A., Vilela, B., & Anderson, R. P. (2015). spThin: An R package for spatial thinning of species occurrence records for use in ecological niche models. Ecography, 38(5), 541–545. https://doi.org/10.1111/ecog.01132

Anderson, R. P., & Gonzalez, I. (2011): Species–specific tuning increases the accuracy of ecological niche models. Ecological Modelling, 222(15), 2796–2811 https://doi.org/10.1016/j.ecolmodel.2011.04.011

AOPK ČR. (2025): Occurrence database of the Nature Conservation Agency of the Czech Republic. Accessed January 2025. Retrieved from https://portal.nature.cz

Araújo, M. B., & Peterson, A. T. (2012): Uses and misuses of bioclimatic envelope modeling. Ecology, 93(7), 1527–1539. https://doi.org/10.1890/11–1930.1

Booth, T. H. (2022): Checking bioclimatic variables that combine temperature and precipitation data before their use in species distribution models. Austral Ecology, 47(7), 1506–1514. https://doi.org/10.1111/aec.13234

Cobos, M. E., Peterson, A. T., Barve, N., & Osorio–Olvera, L. (2019): kuenm: An R package for detailed development of ecological niche models using MaxEnt. PeerJ, 7, e6281. https://doi.org/10.7717/peerj.6281

Elith, J., & Leathwick, J. R. (2009): Species distribution models: Ecological explanation and prediction across space and time. Annual Review of Ecology, Evolution, and Systematics, 40, 677–697. https://doi.org/10.1146/annurev.

ecolsys.110308.120159
Elith, J., Phillips, S. J., Hastie, T., Dudík, M., Chee, Y. E., & Yates, C. J. (2011): A statistical explanation of MaxEnt for ecologists. Diversity and Distributions, 17(1), 43–57. https://doi.org/10.1111/j.1472–4642.2010.00725.x
Franklin, J. (2010): Mapping species distributions: Spatial inference and prediction. Cambridge University Press. https://doi.org/10.1017/CBO9780511810602
GBIF.org (2025): *GBIF Occurrence Download*. Accessed via R package geodata (function sp_occurrence) on 17 January 2025.
Guisan, A., & Thuiller, W. (2005): Predicting species distribution: Offering more than simple habitat models. Ecology Letters, 8(9), 993–1009. https://doi.org/10.1111/j.1461–0248.2005.00792.x
Hijmans, R. J. (2023): raster: Geographic data analysis and modeling (R package version 3.6–26). Retrieved from https://CRAN.R–project.org/package=raster
Hijmans, R. J., Cameron, S. E., Parra, J. L., Jones, P. G., & Jarvis, A. (2023): geodata: R package for downloading geospatial data (R package version 0.5–9). Retrieved from https://CRAN.R–project.org/package=geodata
Kaláb, O. (2024): rndop: Access to the Data from The Species Occurrence Database of NCA CR (Czechia) in R (Version 0.2.1) [Computer software]. https://github.com/kalab-oto/rndop
Karger, D. N., Conrad, O., Böhner, J., Kawohl, T., Kreft, H., Soria–Auza, R. W., Zimmermann, N. E., Linder, H. P., & Kessler, M. (2017): Climatologies at high resolution for the Earth's land surface areas. Scientific Data, 4, 170122. https://doi.org/10.1038/sdata.2017.122
Karger, D. N., Conrad, O., Böhner, J., Kawohl, T., Kreft, H., Soria–Auza, R. W., Zimmermann, N. E., Linder, H. P., & Kessler, M. (2020): CHELSA V2.1: Downscaled climate data. Retrieved from https://chelsa–climate.org/
Lê, S., Josse, J., & Husson, F. (2008): FactoMineR: An R package for multivariate analysis. Journal of Statistical Software, 25(1), 1–18. https://doi.org/10.18637/jss.v025.i01
Lockwood, J. L., Hoopes, M. F., & Marchetti, M. P. (2013): Invasion ecology (2nd ed.). Wiley–Blackwell.
Mesgaran, M. B., Cousens, R. D., & Webber, B. L. (2014): Here be dragons: a tool for quantifying novelty due to covariate range and correlation change when projecting species distribution models. Diversity and Distributions, 20(10), 1147-1159.
Moravcová, L., Pyšek, P., Jarošík, V., & Pergl, J. (2006): Seasonal pattern of germination and seed longevity in the invasive species *Heracleum mantegazzianum*. Preslia, 78, 287–301.
O'Neill, B. C., Kriegler, E., Riahi, K., Ebi, K. L., Hallegatte, S., Carter, T. R., Mathur, R., & van Vuuren, D. P. (2017): The roads ahead: Narratives for Shared Socioeconomic Pathways describing world futures in the 21st century. Global Environmental Change, 42, 169–180. https://doi.org/10.1016/j.gloenvcha.2015.01.004
OpenStreetMap contributors. (2024): OpenStreetMap Standard layer [basemap]. Retrieved via QuickMapServices plugin in QGIS 3.34. Available at: https://www.openstreetmap.org/copyright
Pearson, R. G., & Dawson, T. P. (2003): Predicting the impacts of climate change on the distribution of species: Are bioclimate envelope models useful? Global Ecology and Biogeography, 12(5), 361–371. https://doi.org/10.1046/j.1466–822X.2003.00042.x
Pearson, R. G., Raxworthy, C. J., Nakamura, M., & Peterson, A. T. (2007): Predicting species distributions from small numbers of occurrence records: A test case using cryptic geckos in Madagascar. Journal of Biogeography, 34(1), 102–117. https://doi.org/10.1111/j.1365–2699.2006.01594.x
Phillips, S. J., & Dudík, M. (2008): Modeling of species distributions with MaxEnt: New extensions and a comprehensive evaluation. Ecography, 31(2), 161–175. https://doi.org/10.1111/j.0906–7590.2008.5203.x
Phillips, S. J., Dudík, M., & Schapire, R. E. (n.d.): MaxEnt software for modeling species niches and distributions (Version 3.4.4) [Computer software]. American Museum of Natural History. Retrieved January 21, 2025, from http://biodiversityinformatics.amnh.org/open_source/maxent/
Pyšek, P., Cock, M. J. W., Nentwig, W., & Ravn, H. P. (Eds.). (2007a): Ecology and management of giant hogweed (*Heracleum mantegazzianum*). CABI Publishing. https://doi.org/10.1079/9781845932060.0000
Pyšek, P., Krinke, L., Jarošík, V., Perglová, I., Pergl, J., & Moravcová, L. (2007b): Timing and extent of tissue removal affect reproduction characteristics of an invasive species *Heracleum mantegazzianum*. Biological Invasions, 9(3), 335–351. https://doi.org/10.1007/s10530–006–9038–0
Pyšek, P., Lambdon, P.W., Arianoutsou, M., Kühn, I., Pino, J., Winter, M. (2009): Alien vascular plants of Europe In: Hulme, P.E., Nentwig, W., Pyšek, P., Vilà, M. (eds.) Handbook of alien species in Europe. DAISIE Invading Nature – Springer Series in Invasion Ecology 3 Springer, Dordrecht, 43–61.
QGIS Development Team. (2024): QGIS Geographic Information System. Open geospatial foundation. Retrieved from https://www.qgis.org
R Core Team. (2024): R: A language and environment for statistical computing. R Foundation for Statistical Computing, Vienna, Austria. Retrieved from https://www.R–project.org/
Swets, J. A. (1988): Measuring the accuracy of diagnostic systems. Science, 240(4857), 1285–1293. https://doi.org/10.1126/science.3287615

Thiele, J., & Otte, A. (2007): Impact of *Heracleum mantegazzianum* on invaded vegetation and human activities. In P. Pyšek, M. J. W. Cock, W. Nentwig, & H. P. Ravn (Eds.), Ecology and management of giant hogweed (*Heracleum mantegazzianum*) (pp. 144–156). CABI. https://doi.org/10.1079/9781845932060.0144

Zizka, A., Silvestro, D., Andermann, T., Azevedo, J., Ritter, C. D., Edler, D., Farooq, H., & Antonelli, A. (2019): CoordinateCleaner: Standardized cleaning of occurrence records from biological collection databases. Methods in Ecology and Evolution, 10(5), 744–751. https://doi.org/10.1111/2041–210X.13152

Prediktivní mapy pro druh *Heracleum mantegazzianum* pro období 2011–2040 a 2041–2070 ve střední Evropě.

Tato studie využívá MaxEnt modelování k predikci rozšíření invazní rostliny *H. mantegazzianum* ve střední Evropě (Česká republika, Slovensko, Rakousko, Německo, Polsko) pro období 1980–2010, 2011–2040 a 2041–2070. Pro vytvoření prediktivních map byly použity bioklimatické proměnné z databáze CHELSA 2.1 s rozlišením ~1 km, získané z globálních klimatických modelů CMIP6 (GFDL-ESM4 a IPSL-CM6A-LR) pro dva socioekonomické scénáře (SSP126 a SSP585). Z devatenácti původních proměnných bylo vybráno pět nekorelovaných environmentálních vstev (bio1, bio3, bio4, bio14, bio15). Data o výskytu studovaného druhupocházela z databází AOPK ČR a GBIF, přičemž byla vyčištěna s použitím 1 km parametru pro redukci prostorové autokorelace. Modely byly kalibrovány s 30 000 podkladovými body a dosáhly vysoké přesnosti (Mean AUC ratio 1,324–1,61; chybovost 0,049–0,05). Celkem bylo vytvořeno a vyhodnoceno 1350 modelů, kombinujících různé regularizační parametry, třídy prvků a sady proměnných, přičemž modely pro období 2011–2040 byly promítnuty na klimatické scénáře pro 2041–2070. Pro výpočty byl použit software MaxEnt 3.4.4, R 4.4.2 a QGIS 3.34 „Prizren“. Výsledky ukazují výrazné šíření *H. mantegazzianum* zejména v jižním a západním Německu, s minimálními rozdíly mezi scénáři SSP126 a SSP585. Studie zdůrazňuje potřebu cíleného monitorování a managementu této invazní rostliny vzhledem k dopadům změn klimatu.

Author's address: Lukáš Číhal, Slezské zemské muzeum (Silesian Museum), Nádražní okruh 31, CZ–746 01 Opava, Czech Republic. E–mail: cihal@szm.cz, orcid iD: https://orcid.org/0009–0009–2740–1326